Accepted Manuscript

Lipidomic signature of *Bacillus licheniformis* I89 during the different growth phases unravelled by high-resolution liquid chromatography-mass spectrometry

Celestina Lopes, Joana Barbosa, Elisabete Maciel, Elisabete da Costa, Eliana Alves, Pedro Domingues, Sónia Mendo, M. Rosário M. Domingues

PII: S0003-9861(18)30839-7

DOI: https://doi.org/10.1016/j.abb.2018.12.024

Reference: YABBI 7899

To appear in: *Archives of Biochemistry and Biophysics*

Received Date: 17 October 2018

Revised Date: 4 December 2018

Accepted Date: 21 December 2018

Please cite this article as: C. Lopes, J. Barbosa, E. Maciel, E. da Costa, E. Alves, P. Domingues, Só. Mendo, M.Rosá.M. Domingues, Lipidomic signature of *Bacillus licheniformis* I89 during the different growth phases unravelled by high-resolution liquid chromatography-mass spectrometry, *Archives of Biochemistry and Biophysics* (2019), doi: https://doi.org/10.1016/j.abb.2018.12.024.

This is a PDF file of an unedited manuscript that has been accepted for publication. As a service to our customers we are providing this early version of the manuscript. The manuscript will undergo copyediting, typesetting, and review of the resulting proof before it is published in its final form. Please note that during the production process errors may be discovered which could affect the content, and all legal disclaimers that apply to the journal pertain.

ACCEPTED MANUSCRIPT

Lipidomic signature of *Bacillus licheniformis* I89 during the different growth phases unravelled by high-resolution liquid chromatography-mass spectrometry

Celestina Lopes[1,2,3], Joana Barbosa[2], Elisabete Maciel[1,2,3], Elisabete da Costa[1,3], Eliana Alves[1], Pedro Domingues[1], Sónia Mendo[2], M. Rosário M. Domingues[1,3,*]

[1] Centro de Espectrometria de Massa, Departamento de Química & QOPNA, Universidade de Aveiro, Campus Universitário de Santiago, 3810-193 Aveiro, Portugal

[2] Departamento de Biologia & CESAM, Universidade de Aveiro, 3810-193 Aveiro, Portugal

[3] Departamento de Química & CESAM & ECOMARE, Universidade de Aveiro, 3810-193 Aveiro, Portugal

* Author to whom correspondence should be addressed: M. Rosário M. Domingues; E-mail: mrd@ua.pt

Phone: +351 234 370 698

Fax: +351 234 370 084

ACCEPTED MANUSCRIPT

Abstract

Bacillus licheniformis I89 is a non-pathogenic, Gram-positive bacterium, frequently found in soil. It has several biotechnological applications as producer of valuable compounds such as proteases, amylases, surfactants, and lantibiotics. Herein, it is reported the identification of the polar lipidome of *B. licheniformis* I89 during the different growth phases (lag, exponential and stationary) at 37 ºC. The analytical approach relied on hydrophilic interaction liquid chromatography coupled to electrospray ionization mass spectrometry (HILIC–ESI–MS), accurate mass measurements and tandem mass spectrometry (MS/MS). In the lipidome of *B. licheniformis* I89 were identified four phospholipid classes: phosphatidylethanolamine, phosphatidylglycerol, lysyl-phosphatidylglycerol, and cardiolipin; two glycolipid classes: monoglycosyldiacylglycerol and diglycosyldiacylglycerol; and two phosphoglyceroglycolipid classes: mono-alanylated lipoteichoic acid primer and the lipoteichoic acid primer. The same lipid species were identified at the different growth phases, but there were significant differences on the relative abundance of some molecular species. There was a significant increase in the 30:0 lipids species and a significant decrease in the 32:0 lipid species, between exponential and stationary phases, when compared to lag phase. No differences were observed between exponential and stationary phases. The lipidomic-based approach used herein is a very promising tool to be employed in the study of bacterial lipid composition, which is a requirement to understand its metabolism and response to growth conditions.

Keywords: phospholipid; glycolipid; mass spectrometry; lipidomics; Gram-positive bacteria

ACCEPTED MANUSCRIPT

45

ACCEPTED MANUSCRIPT

1. Introduction

Bacterial membranes are composed mainly by glycerolipids such as phospholipids (PL) and glycolipids (GL) which have an important role in membrane properties and function and are the main lipid players in signalling and regulation events in these organisms [1]. The regulation and homeostasis of membrane lipids is essential to the bacterial growth, differentiation, viability and proliferation [1,2]. Furthermore, lipid metabolism is involved in biological membrane synthesis and energy homeostasis during pathogen replication and resistance [3], since both bacterial lipid composition and lipid organization into domains are important for signalling, secretion, normal physiology, virulence and antibiotic resistance [1]. Despite the importance of lipids in bacterial membranes, many studies focus only on the fatty acid (FA) composition of the membrane of bacteria [4–6]. However, most of the FA in bacteria are esterified to other lipids, namely polar lipids, as PL and GL, that have been mostly overlooked.

Only a few studies reported the lipidome of bacteria. This is possibly due to complexity and distinct types of polar lipids that can be found in different bacteria [7]. Also, the most common analytical methods to study lipids in bacteria, such as thin-layer chromatography (reviewed by [8]), nuclear magnetic resonance [9,10], and gas chromatography (GC) [11], provide limited information. More recently, mass spectrometry (MS)-based approaches have been used for the detailed analysis of the membranes lipidome [12]. These approaches include the direct analysis of the lipid extracts by electrospray ionization (ESI) and matrix-assisted laser desorption/ionization (MALDI) or liquid chromatography (LC) coupled to MS. These lipidomic LC-MS-based approaches have been successfully used to identify a high number of lipids in both Gram-positive and Gram-negative bacteria [13–16].

Direct analysis by ESI-MS of the total lipid extracts of the Gram-positive bacterium *Listeria monocytogenes* identified phosphatidylglycerols (PG), cardiolipins (CL), lysyl-cardiolipins (lys-CL), and diglycosyldiacylglycerols (DGDG) [16]. DGDG and monoglycosyldiacylglycerols (MGDG) were identified in *Streptococcus pneumoniae* [17], and phosphatidic acid (PA), phosphatidylethanolamines (PE), PG and phosphatidylserines (PS) in *Bacillus subtilis* SDB206 [18]. MALDI–MS was also used to study the lipid composition of *B. subtilis* which allowed for the identification of PL and GL classes (PG, PE, lys-PG and DGDG) [19]. An LC–MS-based approach was used for characterizing the lipidome of Gram-positive bacteria including *B. subtilis* [15,18], *Staphylococcus* [14,20] and *Clostridium* [21,22]. LC–MS was used to taxonomically discriminate bacteria from different strains of *Bacillus* and *Brevibacillus*, showing that this can be a promising tool for bacteria classification [23]. Nonetheless, only a few species of PE, lyso-phosphatidylinositol (lyso-PI), and PA were identified [23]. Hydrophilic interaction liquid chromatography coupled to electrospray ionization mass spectrometry (HILIC-ESI-MS) was used to profile the phospholipidome of *Staphylococcus warneri* [14] but, so far, there are no studies using HILIC-ESI-MS in the lipidome analysis of *Bacillus* species.

Bacillus licheniformis is a Gram-positive, endospore-forming bacterium, a non-pathogenic member of the genus *Bacillus*, that belongs to the *B. subtilis* group. It is commonly found in soil and has many biotechnological applications. It produces valuable compounds, such as proteases, amylases, surfactants, immunosuppressors, antimicrobials (*e.g.*, lichenicidin, bacitracin, surfactin), lipids, among others [24,25]. *B. licheniformis* I89 has been described as a lantibiotic (lichenicidin) producer [25]. Lanthipeptides (lanthionine-containing peptides) are ribosomally synthesized and posttranslationally modified peptides (RiPPs). These are natural products with diverse

biological activities, namely antibacterial activity [26]. Considering the potential biotechnological applications of *B. licheniformis* I89, the lipidome of this bacterial strain was characterized by HILIC–ESI–MS at the different growth phases (lag, exponential and stationary) at 37 ºC.

2. Materials and methods

2.1. Bacteria and growth conditions

B. licheniformis I89 was isolated from a hot spring environment from the Azores islands [27]. Liquid cultures were prepared in M medium: 10 g L^{-1} of NaCl, 10 g L^{-1} of tryptone, 5 g L^{-1} of yeast extract, 10 g L^{-1} of KH_2PO_4, with a final pH of 6.5, adjusted with NaOH [28]. An overnight pre-inoculum was prepared to inoculate the medium for total lipid extraction, as follows: a single colony was inoculated in 10 mL of M medium in a 50 mL falcon tube, the cultures were allowed to grow overnight at 37 °C, at 200 rpm, until the OD_{600} reached 0.9. Then, 1 mL of this culture was used to inoculate 100 mL of fresh M medium, in 500 mL Erlenmeyers. Bacterial cells were allowed to grow at 37 °C at 200 rpm, until they reached the lag phase (3 - 4 h incubation, OD_{600} 0.5), the exponential phase (16 h incubation, OD 1.7 – 2.0) and the stationary phase (24 h incubation, OD 1.9 – 2.5). After growth, the cells were harvested at 8000 rpm for 5 min, at room temperature. The supernatants were discarded, and the cellular pellets were stored at -20 ºC until further use. The procedure was done in triplicate for each growth phase at 37 ºC.

2.2. Lipid extraction

The total bacterial lipids were extracted from the pellets previously stored at -20 °C, as described in Alves and co-workers (2013) [14]. Briefly, 6.5 mL of chloroform/methanol (2:1, by volume) were added to the bacterial cells previously suspended in 2 mL of milli-Q water, in glass centrifuge tubes. The mixture was well homogenized by inverting vigorously the tubes several times and incubated on ice for 210 min. The samples were centrifuged at 568 x *g* for 10 min (Mixtasel, JP Selecta S.A., Barcelona, Spain) at room temperature to separate the phases: the aqueous (upper) phase and the organic (lower) phase from which the lipids were obtained. After transferring the organic phase to a clean tube, the extraction was repeated twice from the tube containing the bacterial pellet. The extracts were dried under a nitrogen stream, dissolved in chloroform, transferred to 2 mL amber glass vials and stored under a nitrogen atmosphere at -20 °C until use.

2.3. Quantification of phospholipids by phosphorus assay

The quantification of PL was performed by measuring the phosphorus amount in the total lipid extracts (adapted from [29]). Briefly, lipid hydrolysis was performed by adding 125 µL of 70% perchloric acid to the samples and phosphate standards (100 µg mL^{-1} of sodium phosphate dibasic dihydrate, ranging from 0.10 to 2.00 µg of phosphorus) in glass tubes. The samples incubated 60 min at 180 ºC in a heating block (Block Heater SBH200D/3, Stuart, Bibby Scientific Ltd., Stone, UK), and cooled down to room temperature. Milli-Q water (825 µL), ammonium molybdate (125 µL, 25 g L^{-1} in water), and ascorbic acid (125 µL, 100 g L^{-1} in water) were then added to the samples and standards, homogenizing well between each addition. Samples and standards were, then, incubated for 10 min at 100 °C in a water bath

(Precisterm, JP Selecta S.A., Barcelona, Spain). The absorbance of standards and samples was measured at 797 nm, at room temperature, in a microplate UV-Vis spectrophotometer (Multiskan GO, Thermo Scientific, Hudson, NH, USA).

2.4. Hydrophilic interaction liquid chromatography - electrospray ionization - mass spectrometry (HILIC-ESI-MS)

Polar lipids were analyzed by HILIC-ESI-MS on a Thermo Scientific Accela™ HPLC system with an autosampler online coupled to a Q-Exactive® mass spectrometer with Orbitrap® technology (Thermo Fisher, Scientific, Bremen, Germany). The solvent system consisted of two mobile phases: mobile phase A was acetonitrile/methanol/water, 50:25:25 per volume, with 1 mM ammonium acetate, and mobile phase B was acetonitrile/methanol, 60:40 per volume, with 1mM ammonium acetate. Initially, 0% of mobile phase A was held isocratically for 8 min, followed by a linear increase to 60% of A within 7 min and a maintenance period of 15 min, returning to the initial conditions in 10 min. A volume of 5 µL of each sample containing 5 µg of lipid extract and 95 µL of mobile phase B was introduced into the Ascentis® Si column (15 cm × 1 mm, 3 µm, Sigma-Aldrich) with a flow rate of 40 µL min^{-1} and at 30 ºC. The mass spectrometer was operated simultaneously in positive (electrospray voltage 3.0 kV) and negative (electrospray voltage –2.7 kV) ion modes, with a resolution of 70 000 (FWHM) and automatic gain control (AGC) target of 1 x 10^6. The capillary temperature was 250 ºC and the sheath gas flow was 15 U. In MS/MS experiments, a resolution of 17 500 and AGC target of 1 x 10^5 were used. The cycles consisted in one full scan mass spectrum and ten data-dependent MS/MS scans and were repeated continuously throughout the experiments with the dynamic

exclusion of 60 seconds and intensity threshold of 1 x 10^4. Normalized collision energy™ (CE) ranged between 25, 30 and 35 eV. Data acquisition was carried out using the Xcalibur data system (V3.3, Thermo Fisher Scientific, USA). Three bacterial cultures were analyzed independently for each of the three growth phases. The identification of molecular species of polar lipids was based on the assignment of the molecular ions observed in LC–MS spectra and by the identification of the fragmentation pattern of each class observed in the MS/MS spectrum of each ion [30]. To confirm the identification of molecular species, mass accuracy (Qual Browser) was determined with ≤ 5 ppm.

2.5. Data and Statistical analysis

The raw data were processed using the MZmine software 2.32 [31]. First, the mass list was filtered, followed by peak detection and peak processing. During the processing of the raw data, acquired in full MS mode, only peaks with raw intensity upper than 1e4 and with mass tolerance of 5 ppm were considered. Peak assignment and ion identification based on mass accuracy were performed against an in-house database. Data integration was expressed by the changes of the relative abundance of molecular species of all classes. Variation in the lipidome of *B. licheniformis* I89 was measured in triplicate in three different conditions (lag, exponential and stationary phases). Results were expressed as mean ± SD using one-way analysis of variance (ANOVA) followed by Bonferroni multiple comparison tests to compare the growth phases, after checking for assumptions. Significant differences were determined in relative percentages of molecular species per class (*** $p < 0.001$, ** $p < 0.01$, * $p <$

0.05). Statistical analysis was performed using GraphPad Prism 5.0 for Windows (GraphPad Software, San Diego, CA, USA).

3. Results

The polar lipid profile of *B. licheniformis* I89 was characterized at the molecular level by high-resolution HILIC-ESI-MS, mass accuracy measurements and MS/MS in positive and negative ion modes. The HILIC allowed the separation of several lipid classes (Fig. 1) including PL, GL and phosphoglyceroglycolipids (PGL) (Fig. 2). The lipid species were identified by exact mass measurement and their structural features, as polar head composition and length of the fatty acyl chains, were confirmed by MS/MS spectra interpretation.

3.1. Phospholipid profile

Several classes of PL were identified in *B. licheniformis* I89: PG, lys-PG, CL and PE (Table1).

PG were identified in negative ion mode, as $[M - H]^-$ ions (Fig. 3a), and in positive ion mode, as $[M + NH_4]^+$ ions (Fig. S1a). The most abundant ions seen in the MS spectra of PG, in negative mode (Fig. 3a), were found at *m/z* 721.5, 693.5, and 707.5, corresponding to PG (32:0), PG (30:0), and PG (31:0). The MS/MS spectra of the $[M - H]^-$ ions (Fig. 3b) showed the typical product ion at *m/z* 171.0, assigned as ionized glycerol phosphate polar head, that confirms the presence of a PG molecular species. The MS/MS spectra, in negative mode, provided information about the fatty acyl composition by the identification of the carboxylate anions ($RCOO^-$). The MS/MS spectrum of PG (15:0/17:0) shows the product ions at *m/z* 241.2 and 269.2 corresponding to the carboxylate anions of the C15:0 and C17:0 FA, respectively

(Fig. 3b). These FA were confirmed, as well, by the presence of low abundant product ions at *m/z* 497.3, arising from loss of C15:0 as ketene (-R=C=O) [16]. The *iso* and *anteiso* C15 and C17 are characteristic FA of *Bacillus* spp. [16] and were previously found in the FA profile of these samples analyzed by GC–MS [32]. However, it is not possible to distinguish the linear C15 and C17 from their branched isomers by LC-MS and MS/MS analysis. PG were also identified in the LC-MS/MS data, as $[M + NH_4]^+$ ions (Fig. S1a). The MS/MS of PG (32:0) assigned as PG (15:0/17:0) at *m/z* 740.5 is given as an example (Fig. S1b), showing the combined neutral loss of NH_3 (-17 Da) and the glycerol phosphate polar head (17+ 172 Da), with the formation of the product ion at *m/z* 551.5.

Lys-PG were identified in both negative and positive ion modes, as $[M - H]^-$ and $[M + H]^+$ ions, respectively. In the LC-MS spectra, in negative ion mode, the most abundant species were found at *m/z* 849.6, 821.6, and 835.6, corresponding to lys-PG (32:0), lys-PG (30:0), lys-PG (31:0), respectively. The analysis of the MS/MS spectra of the $[M - H]^-$ ions (Fig. 3a) showed the characteristic product ion at *m/z* 145.1, assigned to the deprotonated lysine. The fatty acyl composition was confirmed by the $[M - H]^-$ ions that showed the typical carboxylate anions ($RCOO^-$). The MS/MS spectrum of lys-PG (32:0), assigned as lys-PG (15:0/17:0) (Fig. 3d) showed the product ions at *m/z* 241.2 and 269.2 assigned as the $RCOO^-$ ions of the FA C15:0 and C17:0, respectively. Lys-PG were also confirmed by MS/MS of the $[M + H]^+$ ions (example of lys-PG (32:0) in Fig. S1d) that showed the typical neutral loss of 300 Da, formed by loss of the polar head group. In this spectrum, it is seen the product ion at *m/z* 301.1, typical of lys-PG class, that corresponds to the protonated lysyl-glycerolphosphate head group.

CL were identified in the LC–MS spectra in negative ion mode as mono-charged ions ($[M - H]^-$, Fig. 3e) and double-charged ions ($[M - 2H]^{2-}$, Fig. S1e). Several molecular species of CL were identified as $[M - H]^-$ ions (Fig. 3e), being the most abundant found at *m/z* 1323.9, 1351.9, 1337.9 and 1309.9, corresponding to CL (62:0), CL (64:0), CL (63:0) and CL (61:0), respectively. The typical fragmentation of CL, as $[M - H]^-$ ions (Fig. 3f), is presented for the MS/MS spectrum of the deprotonated molecule at *m/z* 1323.9, which corresponds to CL (15:0/17:0/15:0/15:0). This spectrum showed the ions at *m/z* 619.4 and 647.5 that correspond to the anions of the PA fragments, $[PA\text{-}(30:0)\text{-}H]^-$ and $[PA(32:0)\text{-}H]^-$, respectively (Fig. 3f). The fatty acyl composition was confirmed by the identification of the $RCOO^-$ product ions at *m/z* 241.2 and 269.2 corresponding to the FA C15:0 and C17:0, respectively. The MS/MS spectrum of the $[M - 2H]^{2-}$ ions (Fig. S1f) of the same CL, at *m/z* 661.5 showed ions at *m/z* 241.2 and 269.2, corresponding to the $RCOO^-$ ions mentioned above.

PE molecular species were identified both in positive and negative ion modes, as $[M + H]^+$ and $[M - H]^-$ ions, respectively (Fig. 3g and Fig. S1g). Several molecular species of PE were identified in positive mode (Fig. 3g) and the most abundant ones were found at *m/z* 692.5, 678.5 and 664.5, corresponding to PE (32:0), PE (31:0), and PE (30:0), respectively. They were confirmed by the analysis of the MS/MS spectra of the $[M + H]^+$ ions by the identification of the typical neutral loss of 141 Da. The MS/MS spectrum of PE (15:0/17:0) (Fig. 3h) showed a product ion at *m/z* 551.5, formed by the loss of the phosphatidylethanolamine head group (-141 Da) from the precursor $[M + H]^+$ ion at *m/z* 692.3. The fatty acyl composition was confirmed by the analysis of the MS/MS spectra of the $[M - H]^-$ ions that showed the typical

carboxylate anions ($RCOO^-$). Fig. S1h shows the $RCOO^-$ at *m/z* 241.2 and 269.2, that correspond to the FA C15:0 and C17:0, respectively.

3.2. Glycolipid profile

Two glycolipid classes were assigned in the lipidome of *B. licheniformis* I89: MGDG and DGDG (Table 2).

MGDG were identified as $[M + NH_4]^+$ (Fig. 4a). The most abundant MGDG species were found at *m/z* 748.6, 734.6 and 720.6, assigned to MGDG (32:0), MGDG (31:0), and MGDG (30:0), respectively. These lipids were confirmed by MS/MS analysis in positive ion mode (Fig. 4b) by the identification of the typical neutral loss of 197 Da, corresponding to the combined loss of a hexose (-180 Da) and the loss of NH_3 (-17 Da). Fig. 4b shows, as an example of the fragmentation of this class of GL, the MS/MS spectrum of MGDG (15:0/17:0), at *m/z* 748.6, that showed a product ion at *m/z* 551.5 formed by the loss of hexose combined with the loss of NH_3. The fatty acyl composition was confirmed by the presence of product ions at *m/z* 299.3, corresponding to the ion C15:0 (242 Da) plus the glycerol moiety (57 Da). Also, at *m/z* 327.3 corresponding to the C17:0 plus 57 Da, also designated $[RCO+74]^+$ ions [33].

DGDG were identified (Fig. 4c). The most abundant DGDG molecular species were seen in the LC-MS data at *m/z* 910.6, 896.6 and 882.6 that corresponded to DGDG (32:0), DGDG (30:0) and DGDG (31:0), respectively. They were confirmed by MS/MS analysis by the identification of the typical neutral loss of 359 Da arising from the loss of two hexoses (loss of 162+180 Da) combined with the loss of NH_3 (-17 Da). This typical fragmentation pathway can be observed in Fig. 4d, showing the

MS/MS spectrum of DGDG (17:0/15:0) at *m/z* 910.6, that led to the formation of the product ion at *m/z* 551.5. The fatty acyl composition was confirmed by the presence of the acylium ions plus 74 ($[RCO+74]^+$), as described for the MGDG class. In the case of DGDG (17:0/15:0) (Fig. 4d), these product ions can be seen at *m/z* 299.3 that corresponds to $[RCO+74]^+$ of C15:0, and at *m/z* 327.3 that corresponds to $[RCO+74]^+$ of C17:0.

Neutral glycolipids MGDG and DGDG were also detected in LC-MS in negative ion mode as $[M + CH_3COO]^-$ ions (Fig. S2a and S2c). They were confirmed by mass accuracy (Table 2) and by MS/MS analysis that showed only the carboxylate anions $RCOO^-$, and not the loss of the sugar moieties (Fig. S2b and S2d).

3.3. Phosphoglyceroglycolipid profile

PGL, well known glycolipid anchors of lipoteichoic acid [34], were identified in *B. licheniformis* I89 as mono-alanylated lipoteichoic acid primer (LTAP-Ala) and the lipoteichoic acid primer (LTAP) (Table 3).

LTAP were identified in negative ion mode as $[M - H]^-$ ions (Fig. 5a). The most abundant molecular species were found at *m/z* 1045.6, 1031.6 and 1017.6, assigned as LTAP (32:0), LTAP (31:0), LTAP (30:0), respectively. The MS/MS spectra of this class (Fig. 5b) showed the typical product ions: at *m/z* 79.0, that corresponds to deprotonate ion of the phosphate residue; at *m/z* 153.0, that corresponds to the glycerolphosphate residue; and at *m/z* 171.0, that corresponds to glycerolphosphate. These product ions can be observed in the MS/MS spectrum of the $[M - H]^-$ ion of LTAP (15:0:/15:0) at *m/z* 1017.6 (Fig. 5b). FA were identified by the presence of the $RCOO^-$ ions at *m/z* 241.2 corresponding to C15:0.

LTA-Ala were identified in negative ion mode, as $[M - H]^-$ ions (Fig. 5c) and confirmed by MS/MS analysis (Fig. 5d). The molecular species identified were found at *m/z* 1116.6, 1088.6 and 1102.6, assigned as LTAP-Ala(32:0), LTAP-Ala(30:0), LTAP-Ala(31:0), respectively. This class was identified by the typical neutral loss of alanine (-89 Da), and the product ion at *m/z* 88.0 that corresponds to the anion of the terminal ester linked alanine [34]. The product ions at *m/z* 79.0 and at *m/z* 153.0 were also observed and confirmed the presence of phosphate and glycerophosphate moieties, respectively. The FA composition was confirmed by the identification of the $RCOO^-$ ions at *m/z* 241.2 and 269.2 that matched with the expected LTA-Ala (15:0/17:0) composition.

3.4. Lipid profile is growth phase-dependent

The lipid profile was analyzed in the three growth phases: lag, exponential and stationary, at 37 °C. The same lipid classes and molecular species were identified in all growth phases, but there were changes in the relative abundances of the lipid species in all PL classes. Significant differences in PG molecular species were observed for PG (30:0) and PG (32:0) ($p < 0.001$, ANOVA) and PG (31:0) ($p < 0.05$, ANOVA) (Fig. 6a). PG (30:0) significantly increased along the growth phases while PG (32:0) decreased from the lag to the exponential and stationary phase. PG (31:0) decreased in stationary phase (Fig. 6a). As for PG, significant differences in the relative abundance of lys-PG (32:0) and lys-PG (30:0) were observed ($p < 0.001$, ANOVA) (Fig. 6b). Lys-PG (30:0) increased over the growth phases, while lys-PG (32:0) decreased from the lag to the stationary phases. Significant differences in CL molecular species were observed for CL (64:0) (Fig. 6c). The CL (64:0) decreased

from the lag to the exponential phase and increased from the exponential to the stationary phase. The differences in the relative abundance of PE occurred in PE (30:0) and PE (32:0) (Fig. 6d). PE (30:0) increased along the growth phases, while PE (32:0) decreased throughout the growth phases.

For the GL, significant differences in the relative abundance of MGDG were observed in MGDG (30:0) which increased from the lag phase to the stationary phase (Fig. 6e). Significant differences were observed in the relative abundance of DGDG (30:0) and DGDG (32:0) (Fig. 6f). DGDG (30:0) increased throughout the growth phases the lag to stationary growth phases, while DGDG (32:0) decreased (Fig. 6f).

Regarding PGL classes, the differences in the relative abundances occurred in LTAP (32:0) (Fig. 6g), that decreased from the lag to the exponential phase and increased from the exponential to the stationary phase. The differences in LTAP-Ala class occurred in LTAP-Ala (30:0) ($p < 0.001$, ANOVA) and LTAP-Ala (32:0) ($p < 0.05$, ANOVA) (Fig. 6h). LTAP-Ala (30:0) increased throughout the growth phases and LTAP-Ala (32:0) decreased throughout the phases.

4. Discussion

Membrane lipid homeostasis and adaptation to changing environmental conditions are essential for bacterial survival [1]. Lipid metabolism and lipid profile can change depending on growth conditions, such as temperature [35]. Modifications in the lipid composition of bacterial membrane were associated with changes in the profile of FA or the ratio of *iso* to *anteiso* chains [35]. Also, it is known that changes in the lipid composition, not only at the FA level but also in the PL and GL profiles, can affect membrane properties, bacterial survival and pathogenicity [36]. However, the lipidome of most bacteria is still unknown [1].

The polar lipidome of *B. licheniformis* I89 was studied herein. Polar lipids were extracted and analyzed, both in negative and positive ion modes, by means of an LC-MS-based lipidomic platform. This approach allowed for the identification of several classes of polar lipids providing a more complete lipidomic signature of this bacterial strain. Previous studies performed in *Bacillus* spp. could identify only three PL classes (PG, PE and lys-PG) and one GL class (DGDG) [19]. In this study, four PL classes, two GL classes, and two PGL classes were identified. The PL classes identified in *B. licheniformis* I89 were PG, PE, lys-PG, and CL. These lipid classes were already reported in other studies of *Bacillus* spp. and also of other Gram-positive bacteria. However, CL and PE classes have never been reported in the lipidome of *B. licheniformis*, contrarily to PG and lys-PG [23]. CL is a universal component of energy generating membranes, it plays an important function in diverse physiological processes, including stability and localization of proteins and protein complexes, formation of membrane microdomains and the production of membrane potential [37]. Besides, CL exhibits a cone-shaped architecture that locates at regions of negative membrane curvature [38,39] responsible for modulating membrane properties and function, and protein location in the cellular membrane.

Lys-PG are aminoacylated PG commonly present in bacterial cytoplasmic membranes and have a key role in the stabilization of the membranes [40]. In *S. aureus*, they seem to play a role in the resistance to cationic antimicrobial peptides and to the lipopeptide antibiotic daptomycin. This effect seems to be related with the decreased susceptibility of the membrane to these compounds due to the partial neutralization of the cellular membrane by the cationic headgroup of lys-PG [41]. These membrane lipids also provide protection against bacitracin, aminoglycosides, and some β-lactams [42].

DGDG were already identified in members of the *Bacillu*s spp. and other Gram-positive bacteria [19,43,44]. MGDG were reported in other Gram-positive bacteria [17] but not in the lipidome of *B. licheniformis* or another *Bacillu*s spp.

Lipoteichoic acid (LTA) and alanyl-lipoteichoic acid (Ala-LTA) classes, identified in this study, were already reported in Gram-positive bacteria, including *Bacillus spp*. Aminoacylated lipids were shown to play a role in surface charge modulation of Gram-positive bacteria [45]. LTA are recognized as immunomodulating effector molecules and can induce an *in vitro* pro-inflammatory response in immune cells [46]. This response occurs due to D-alanyl substitution of the LTA backbone, its glycolipid anchor [47,48]. Thus, the absence of functional LTA in the bacterial membrane improves the bacterial anti-inflammatory ability [46,49].

The polar lipid profile described in this study for *B. licheniformis* I89 agrees with data reported previously for Gram-positive bacteria and for some *Bacillus* species, but those works reported only few groups of lipids in the bacteria [16,19,50]. Gram-positive bacteria are known to contain PL bearing amino acids in the head group, such as lysine, alanine and ornithine [51]. DGDG and MGDG were reported for other *Bacillus* spp., identified by TLC or by direct MS analysis [18,23].

The identification of the polar lipidome of bacteria is important to provide information about their adaptation mechanisms, namely to developing antibiotic resistance. Previous studies reported a correlation between lipid composition and antibiotic resistance in bacteria [50,52]. In *Enterococcus faecalis*, a Gram-positive, opportunistic, pathogenic bacterium [50], antibiotic resistance was correlated with a decrease in PG and lys-PG levels which, most probably, provide resistance to cationic antimicrobial peptides [50]. Changes in PL profile were also observed in MG1655, DPB635 and DPB636 *E. coli* strains, after exposure to the antibiotic norfloxacin, with

up regulation of FA and down regulation of glycerophospholipids [52]. Other works reported that the susceptibility to different antibiotics in the pathogenic bacteria *Staphylococcus haemolyticus* and *Staphylococcus epidermidis* depends on the variations of the lipidome induced by nutrition depletion [53].

5. Conclusions

The profiling of the polar lipidome of *Bacillus* species and other Gram-positive bacteria by LC-MS is still in its infancy. In the lipidome of *B. licheniformis* I89, one hundred and fourteen molecular species of polar lipids by LC-MS were identified and structurally characterized, comprising phospholipids (PG, lys-PG, PE, and CL), glycolipids (MGDG, DGDG), and phosphoglyceroglycolipids (LTAP, LTA-Ala). Membrane lipid composition of this strain is significantly modified during the different growth phases. Thus, the results in the present work obtained through LC-MS with high resolution MS are promising to understand the adaptation of the lipid metabolism of *Bacillus,* under different growth conditions, that can be useful to understand mechanisms of resistance and also for taxonomy classification.

Conflicts of interest

None.

Appendix A. Supplementary data

Acknowledgment

ACCEPTED MANUSCRIPT

Thanks are due to University of Aveiro, Fundação para a Ciência e a Tecnologia (FCT)/MEC, European Union, QRN, COMPETE for the financial support to the Organic Chemistry, Natural and Agrofood Products (QOPNA) research Unit (FCT UID/QUI/00062/2013), Portuguese Mass Spectrometry Network, RNEM (LISBOA-01-0145-FEDER-402-022125) and Centre for Environmental and Marine Studies (CESAM) (UID/AMB/50017/2013), through national founds and where applicable co-financed by the FEDER, within the PT2020 Partnership Agreement, and also to the Portuguese Mass Spectrometry Network (REDE/1504/REM/2005). Celestina Lopes is grateful to Calouste Gulbenkian Foundation for her PhD grant (process number 135624). Joana Barbosa (SFRH/BD/97099/2013), Elisabete Maciel (SFRH/BPD/104165/2014), Elisabete da Costa (SFRH/BD/52499/2014) and Eliana Alves (SFRH/BPD/109323/2015) are grateful to FCT for their grants.

References

[1] C. Sohlenkamp, O. Geiger, Bacterial membrane lipids: Diversity in structures and pathways, FEMS Microbiol. Rev. 40 (2015) 133–159 https//doi.org/10.1093/femsre/fuv008.

[2] J.B. Parsons, C.O. Rock, Bacterial lipids: Metabolism and membrane homeostasis, Prog. Lipid. Res. 52 (2013) 249–276 https//doi.org/10.1016/j.plipres.2013.02.002.

[3] M.R. Wenk, Lipidomics of host-pathogen interactions, FEBS Lett. 580 (2006) 5541–5551 https//doi.org/10.1016/j.febslet.2006.07.007.

[4] J. Beranová, M.J. Rzemińska, D. Elhottová, K. Strzałka, I. Konopásek, Metabolic control of the membrane fluidity in *Bacillus subtilis* during cold

456 adaptation, Biochim. Biophys. Acta - Biomembr. 1778 (2008) 445–453
457 https//doi.org/10.1016/j.bbamem.2007.11.012.

458 [5] J. Sikorski, E. Brambilla, R.M. Kroppenstedt, B.J. Tindall, The temperature-
459 adaptive fatty acid content in *Bacillus simplex* strains from "Evolution
460 Canyon", Israel, Microbiol. 154 (2008) 2416–2426
461 https//doi.org/10.1099/mic.0.2007/016105-0.

462 [6] Y.G. Chen, F.L. Gu, J.H. Li, F. Xu, S.Z. He, Y.M. Fang, *Bacillus vanillea* sp.
463 nov., isolated from the cured vanilla bean, Curr. Microbiol. 70 (2015) 235–239
464 https//doi.org/10.1007/s00284-014-0707-4.

465 [7] E. Layre, D.B. Moody, Lipidomic profiling of model organisms and the
466 world's major pathogens, Biochimie 95 (2013) 109–115
467 https://doi.org/10.1016/j.biochi.2012.08.012

468 [8] B. Fuchs, R. Süß, K. Teuber, M. Eibisch, J. Schiller, Lipid analysis by thin-
469 layer chromatography-A review of the current state, J. Chromatogr. A. 1218
470 (2011) 2754–2774 https//doi.org/10.1016/j.chroma.2010.11.066.

471 [9] J. Sauvageau, J. Ryan, K. Lagutin, I.M. Sims, B.L. Stocker, M.S.M. Timmer,
472 Isolation and structural characterisation of the major glycolipids from
473 *Lactobacillus plantarum*, Carbohydr. Res. 357 (2012) 151–156
474 https//doi.org/10.1016/j.carres.2012.05.011.

475 [10] T.L. Palama, I. Canard, G.J.P. Rautureau, C. Mirande, S. Chatellier, B.E.
476 Herrmanna, Identification of bacterial species by untargeted NMR
477 spectroscopy of the exo-metabolome, Analyst. 141 (2016) 4558–4561
478 https//doi.org/10.1039/C6AN00393A.

479 [11] M.A. Haque, N.J. Russell, Strains of *Bacillus cereus* vary in the phenotypic

adaptation of their membrane lipid composition in response to low water activity, reduced temperature and growth in rice starch, Microbiol. 150 (2004) 1397-404 https//doi.org/10.1099/mic.0.26767-0.

[12] R. Harkewicz, E.A. Dennis, Applications of mass spectrometry to lipids and membranes, Annu. Rev. Biochem. 80 (2012) 301–325. https//doi.org/10.1146/annurev-biochem-060409-092612.

[13] T. Kondakova, N. Merlet-Machour, M. Chapelle, D. Preterre, F. Dionnet, M. Feuilloley, N. Orange, C. Duclairoir Poc, A new study of the bacterial lipidome: HPTLC-MALDI-TOF imaging enlightening the presence of phosphatidylcholine in airborne *Pseudomonas fluorescens* MFAF76a, Res. Microbiol. 166 (2015) 1–8 https//doi.org/10.1016/j.resmic.2014.11.003.

[14] E. Alves, T. Melo, C. Simões, M.A.F. Faustino, J.P.C. Tomé, M.G.P.M.S. Neves, J.A.S. Cavaleiro, Â. Cunha, N.C.M. Gomes, P. Domingues, M.R.M. Domingues, A. Almeida, Photodynamic oxidation of *Staphylococcus warneri* membrane phospholipids: new insights based on lipidomics, Rapid. Commun. Mass. Spectrom. 27 (2013) 1607–1618 https//doi.org/10.1002/rcm.6614.

[15] P. Bernat, K. Paraszkiewicz, P. Siewiera, M. Moryl, G. Płaza, J. Chojniak, Lipid composition in a strain of *Bacillus subtilis*, a producer of iturin A lipopeptides that are active against uropathogenic bacteria, World J. Microbiol. Biotechnol. 32 (2016) 1-13 https//doi.org/10.1007/s11274-016-2126-0.

[16] R.V.V. Tatituri, B.J. Wolf, M.B. Brenner, J. Turk, F.F. Hsu, Characterization of polar lipids of *Listeria monocytogenes* by HCD and low-energy CAD linear ion-trap mass spectrometry with electrospray ionization, Anal. Bioanal. Chem. 407 (2015) 2519–2528 https//doi.org/10.1007/s00216-015-8480-1.

[17] R.V.V. Tatituri, M.B. Brenner, J. Turk, F.F. Hsu, Structural elucidation of diglycosyl diacylglycerol and monoglycosyl diacylglycerol from *Streptococcus pneumoniae* by multiple-stage linear ion-trap mass spectrometry with electrospray ionization, J. Mass Spectrom. 47 (2013) 115–123 https//doi.org/10.1002/jms.2033.

[18] V.M. Bierhanzl, R. Čabala, M. Ston, P. Kotora, V. Ferenczy, J. Blaško, R. Kubinec, G. Seydlová, Direct injection mass spectrometry, thin layer chromatography, and gas chromatography of *Bacillus subtilis* phospholipids, Monats Chem. 147 (2016) 1385–1391 https//doi.org/10.1007/s00706-016-1734-6.

[19] J. Gidden, J. Denson, R. Liyanage, D.M. Ivey, J.O. Lay, Lipid compositions in *Escherichia coli* and *Bacillus subtilis* during growth as determined by MALDI-TOF and TOF/TOF mass spectrometry, Int. J. Mass Spectrom. 283 (2009) 178–184 https//doi.org/10.1016/j.ijms.2009.03.005.

[20] W.H. Belka, J. Nakonieczna, M.Belka, T.Baczek, J.Namieśnik, A.K. Wasik, Comprehensive methodology for *Staphylococcus aureus* lipidomics by liquid chromatography and quadrupole time-of-flight mass spectrometry, J. Chromatogr. A. 1362 (2014) 62–74 https//doi.org/10.1016/j.chroma.2014.08.020.

[21] Z. Guan, N.C. Johnston, S. Aygun-Sunar, F. Daldal, C.R.H. Raetz, H. Goldfine, Structural characterization of the polar lipids of *Clostridium novyi* NT. Further evidence for a novel anaerobic biosynthetic pathway to plasmalogens, Biochim. Biophys. Acta 1811 (2011) 186–193 https//doi.org/10.1016/j.bbalip.2010.12.010.

528 [22] Z. Guan, N.C. Johnston, C.R.H. Raetz, E.A. Johnson, H. Goldfine, Lipid
529 diversity among botulinum neurotoxin-producing clostridia, Microbiol. 158
530 (2012) 2577–2584 https//doi.org/10.1099/mic.0.060707-0.

531 [23] N. Almasoud, Y. Xu, D.K. Trivedi, S. Salivo, T. Abban, N.J.W. Rattray, E.
532 Szula, H. AlRabiah, A. Sayqal, R. Goodacre, Classification of *Bacillus* and
533 *Brevibacillus* species using rapid analysis of lipids by mass spectrometry, Anal.
534 Bioanal. Chem. 408 (2016) 7865–7878 https//doi.org/10.1007/s00216-016-
535 9890-4.

536 [24] T. Stein, *Bacillus subtilis* antibiotics: structures, syntheses and specific
537 function, Mol. Microbiol. 56 (2005) 845–857 https//doi.org/10.1111/j.1365-
538 2958.2005.04587.x.

539 [25] T. Caetano, J.M. Krawczyk, E. Mösker, R.D. Süssmuth, S. Mendo,
540 Heterologous expression, biosynthesis, and mutagenesis of type II lantibiotics
541 from *Bacillus licheniformis* in *Escherichia coli*, Chem. Biol. 18 (2011) 90–100
542 https//doi.org/10.1016/j.chembiol.2010.11.010.

543 [26] Q. Zhang, J.R. Doroghazi, X. Zhao, M.C. Walker, W.A. van der Donk,
544 Expanded natural product diversity revealed by analysis of lanthipeptide-like
545 gene clusters in Actinobacteria, Appl. Environ. Microbiol. 81 (2015) 4339–
546 4350 https//doi.org/10.1128/AEM.00635-15.

547 [27] S.A.L. V Mendo, I.S. Henriques, A.C.M. Correia, J.M.C. Duarte, Genetic
548 characterization of a new thermotolerant *Bacillus licheniformis* strain, Curr.
549 Microbiol. 40 (2000) 137–139 https//doi.org/10.1007/s002849910028.

550 [28] S. Mendo, N.A. Faustino, A.C. Sarmento, F. Amado, A.J.G. Moir, Purification
551 and characterization of a new peptide antibiotic produced by a thermotolerant

Bacillus licheniformis strain, Biotechnol. Lett. 26 (2004) 115–119 https//doi.org/10.1023/B:BILE.0000012888.72489.3f.

[29] E.M. Bartlett, D.H. Lewis, Spectrophotometric determination of phosphate esters in the presence and absence of orthophosphate, Anal. Biochem. 36 (1970) 159–167 https//doi.org/10.1016/0003-2697(70)90343-X.

[30] E. Da Costa, T. Melo, A.S.P. Moreira, C. Bernardo, L. Helguero, I. Ferreira, M.T. Cruz, A.M. Rego, P. Domingues, R. Calado, M.H. Abreu, M.R. Domingues, Valorization of lipids from *Gracilaria* sp. through lipidomics and decoding of antiproliferative and anti-inflammatory activity, Mar. Drugs. 15 (2017) 1-17 https//doi.org/10.3390/md15030062.

[31] T. Pluskal, S. Castillo, S., A.V. Briones, M. Oresic, MZmine 2: modular framework for processing, visualizing, and analyzing mass spectrometry-based molecular profile data. *BMC Bioinformatics* 11 (2010) 1-11 https//doi.org/ 10.1186/1471-2105-11-395.

[32] C. Lopes, J. Barbosa, E. Maciel, E. da Costa, E. Alves, F. Ricardo, P. Domingues, S. Mendo, M. R. M. Domingues, Unraveling fatty acid profile of *Bacillus licheniformis* I89 in response to changes in growth conditions fostering new biotechnological applications. Lipids. Under review. Manuscript ID LIPIDS-18-0183.

[33] R.C. Murphy, Tandem mass spectrometry of lipids: Molecular analysis of complex lipids, 4th ed, Royal Society of Chemistry, Science Park, Milton Road UK, 2014.

[34] Y. Luo, Alanylated lipoteichoic acid primer in *Bacillus subtilis*, F1000Res. 5 (2016) 1-19 https//doi.org/10.12688/f1000research.8007.1.

576 [35] Y. Zhang, C.O. Rock, Membrane lipid homeostasis in bacteria, Nat. Rev.
577 Microbiol. 6 (2008) 222–233 https//doi.org/10.1038/nrmicro1839.

578 [36] C. Slavetinsky, S. Kuhn, A. Peschel, Bacterial aminoacyl phospholipids –
579 biosynthesis and role in basic cellular processes and pathogenicity, Biochim.
580 Biophys. Acta 1862 (2017) 1310–1318
581 https//doi.org/10.1016/j.bbalip.2016.11.013.

582 [37] L.D. Renner, D.B. Weibel, Cardiolipin microdomains localize to negatively
583 curved regions of *Escherichia coli* membranes, Proc. Natl. Acad. Sci. USA 108
584 (2011) 6264-6269 https//doi.org/ 10.1073/pnas.1015757108

585 [38] E. Mileykovskaya, W. Dowhan, Visualization of phospholipid domains in
586 *Escherichia coli* by using the cardiolipin-specific fluorescent dye 10-N-Nonyl
587 acridine orange, J. Bacteriol. 182 (2000) 1172-1175
588 https//doi.org/10.1128/JB.182.4.1172-1175.2000

589 [39] P.M. Oliver, J. A. Crooks, M. Leidl, E. J. Yoon, A. Saghatelian, D. B. Weibel,
590 Localization of anionic phospholipids in *Escherichia coli* cells, J. Bacteriol.
591 196 (2014) 3386–3398 https//doi.org/10.1128/JB.01877-14

592 [40] E. Cox, A. Michalak, S. Pagentine, P. Seaton, A. Pokorny, Lysylated
593 phospholipids stabilize models of bacterial lipid bilayers and protect against
594 antimicrobial peptides, Biochim. Biophys. Acta - Biomembr. 1838 (2014)
595 2198–2204 https//doi.org/10.1016/j.bbamem.2014.04.018.

596 [41] A. Peschel, R.W. Jack, M. Otto, L.V. Collins, P. Staubitz, G. Nicholson, H.
597 Kalbacher, et al, *Staphylococcus aureus* resistance to human defensins and
598 evasion of neutrophil killing via the novel virulence factor Mprf is based on
599 modification of membrane lipids with l-lysine, J. Exp. Med. 193 (2001) 1067–

1076 https//doi.org/10.1084/jem.193.9.1067.

[42] H. Nishi, H. Komatsuzawa, T. Fujiwara, N. McCallum, M. Sugai, Reduced content of lysyl-phosphatidylglycerol in the cytoplasmic membrane affects susceptibility to moenomycin, as well as vancomycin, gentamicin, and antimicrobial peptides, in *Staphylococcus aureus*, Antimicrob. Agents Chemother. 48 (2004) 4800–4807 https//doi.org/10.1128/AAC.48.12.4800-4807.2004.

[43] J.D. Kornspan, S. Rottem, The phospholipid profile of Mycoplasmas, J. Lipids. 2012 (2012) 1–8 https//doi.org/10.1155/2012/640762.

[44] M. Meiers, C. Volz, J. Eisel, P. Maurer, B. Henrich, R. Hakenbeck, Altered lipid composition in *Streptococcus pneumoniae* cpoA mutants, BMC Microbiol. 14 (2014) 1-12 https//doi.org/10.1186/1471-2180-14-12.

[45] H. Roy, Tuning the properties of the bacterial membrane with aminoacylated phosphatidylglycerol, IUBMB Life 61 (2009) 940–953 https//doi.org/10.1002/iub.240.

[46] C. Grangette, S. Nutten, E. Palumbo, S. Morath, C. Hermann, J. Dewulf, et al., Enhanced antiinflammatory capacity of a *Lactobacillus plantarum* mutant synthesizing modified teichoic acids., Proc. Natl. Acad. Sci. USA 102 (2005) 10321–6 https//doi.org/10.1073/pnas.0504084102.

[47] C. Rockel, T. Hartung, C. Hermann, Different *Staphylococcus aureus* whole bacteria mutated in putative pro-inflammatory membrane components have similar cytokine inducing activity, Immunobiol. 216 (2011) 316–321 https//doi.org/10.1016/j.imbio.2010.08.001.

[48] J.M. Wells, Immunomodulatory mechanisms of lactobacilli, Microb. Cell Fact.

624 10 (2011) S17 https//doi.org/10.1186/1475-2859-10-S1-S17.

625 [49] I.J.J. Claes, S. Lebeer, C. Shen, T.L.A. Verhoeven, E. Dilissen, G. De Hertogh,
626 et al., Impact of lipoteichoic acid modification on the performance of the
627 probiotic *Lactobacillus rhamnosus* GG in experimental colitis, Clin. Exp.
628 Immunol. 162 (2010) 306–314 https//doi.org/10.1111/j.1365-
629 2249.2010.04228.x.

630 [50] R. Rashid, A. Cazenave-Gassiot, I.H. Gao, Z.J. Nair, J.K. Kumar, L. Gao, K.A.
631 Kline, M.R. Wenk, Comprehensive analysis of phospholipids and glycolipids
632 in the opportunistic pathogen *Enterococcus faecalis*, PLoS One. 12 (2017) 1–
633 20 https//doi.org/10.1371/journal.pone.0175886.

634 [51] C. Sohlenkamp, K.A. Galindo-Lagunas, Z. Guan, P. Vinuesa, S. Robinson, J.
635 Thomas-Oates, C.R.H. Raetz, O. Geiger, The lipid lysyl-phosphatidylglycerol
636 is present in membranes of *Rhizobium tropici* CIAT899 and confers increased
637 resistance to polymyxin B under acidic growth conditions, Mol. Plant-Microbe
638 Interact. 20 (2007) 1421–1430 https//doi.org/10.1094/MPMI-20-11-1421.

639 [52] E. R. Schenk, F. Nau, C. J. Thompson, Y. C. Dinh, and F.F.-Lima, Changes in
640 lipid distribution in *E. coli* strains in response to norfloxacin, J. Mass Spectrom.
641 50 (2015) 88–94 10.1002/jms.3500

642 [53] Y. Luo, M.A. Javed, H. Deneer, Comparative study on nutrient depletion-
643 induced lipidome adaptations in *Staphylococcus haemolyticus* and
644 *Staphylococcus epidermidis*, Sci. Rep. 8 (2018) 1-10
645 https//doi.org/10.1038/s41598-018-20801-7.

646

647 **Tables**

648

649 Table 1. Molecular species of phospholipids from *B. licheniformis* I89 identified by

650 LC-MS in positive and negative ion modes

	Mass spectrometry data			
Lipid Group	Observed *m/z* value	Calculated *m/z* value	Mass deviation [ppm]	Fatty acid chains
Phosphatidylglycerols $[M - H]^-$				
PG (28:0)	665.4394	665.4394	0.0556	13:0/15:0; 14:0/14:0
PG (29:0)	679.4543	679.4550	-1.0494	15:0/14:0; 13:0/16:0
PG (30:0)	693.4703	693.4707	-0.5235	15:0/15:0; 14:0/16:0
PG (31:1)	705.4687	705.4707	-2.7825	15:0/16:1
PG (31:0)	707.4860	707.4863	-0.4424	15:0/16:0; 14:0/17:0
PG (32:1)	719.4844	719.4863	-2.6588	15:0/17:1; 15:1/17:0; 16:1/16:0
PG (32:0)	721.5019	721.5020	-0.0859	15:0/17:0; 16:0/16:0
PG (33:0)	735.5170	735.5176	-0.8334	18:0/15:0; 16:0/17:0; 19:0/14:0
PG (34:1)	747.5140	747.5176	-4.8333	16:1/18:0; 17:1/17:0; 16:0/18:1
PG (34:0)	749.5327	749.5333	-0.7511	19:0/15:0; 17:0/17:0
PG (35:0)	763.5484	763.5489	-0.6719	18:0/17:0; 15:0/20:0
Lysyl phosphatidylglycerols $[M - H]^-$				
lys-PG (29:0)	807.5502	807.5500	0.2774	14:0/15:0
lys-PG (30:0)	821.5659	821.5656	0.3335	15:0/15:0; 14:0/16:0
lys-PG (31:1)	833.5662	833.5656	0.6886	15:0/16:1
lys-PG (31:0)	835.5812	835.5813	-0.0910	15:0/16:0; 17:0/14:0
lys-PG (32:1)	847.5810	847.5813	-0.3256	15:0/17:1
lys-PG (32:0)	849.5965	849.5969	-0.5002	15:0/17:0; 16:0/16:0
lys-PG (33:0)	863.6123	863.6126	-0.3196	16:0/17:0; 15:0/18:0
lys-PG (34:0)	877.6277	877.6282	-0.5993	17:0/17:0; 15:0/19:0
Phosphatidylethanolamines $[M - H]^-$				
PE (28:0)	634.4456	634.4448	1.2893	15:0/13:0; 14:0/14:0
PE (29:0)	648.4606	648.4604	0.2591	15:0/14:0
PE (30:1)	660.4609	660.4604	0.7086	15:1/15:0; 14:0/16:1; 14:1/16:0
PE (30:0)	662.4766	662.4761	0.7819	15:0/15:0; 14:0/16:0
PE (31:1)	674.4759	674.4761	-0.2698	15:0/16:1
PE (31:0)	676.4916	676.4917	-0.1951	15:0/16:0; 14:0/17:0
PE (32:1)	688.4918	688.4917	0.0988	15:0/17:1; 16:1/16:0
PE (32:0)	690.5073	690.5074	-0.1188	15:0/17:0; 16:0/16:0
PE (33:2)	700.4920	700.4917	0.3826	15:0/18:2

ACCEPTED MANUSCRIPT

PE (33:1)	702.5063	702.5074	-1.5402	15:0/18:1; 16:0/17:1; 17:0/16:1
PE (33:0)	704.5224	704.5230	-0.8971	15:0/18:0; 17:0/16:0
PE (34:1)	716.5206	716.5230	-3.3942	18:1/16:0; 16:1/18:0
PE (34:0)	718.5385	718.5387	-0.2533	17:0/17:0; 15:0/19:0; 16:0/18:0
Cardiolipins $[M - H]^-$				
CL (60:0)	1295.8987	1295.9018	-2.3968	15:0/15:0/15:0/15:0
CL (61:0)	1309.9151	1309.9175	-1.7986	15:0/15:0/16:0/15:0
CL (62:0)	1323.9309	1323.9331	-1.6662	15:0/15:0/15:0/17:0; 15:0/16:0/15:0/16:0; 14:0/17:0/16:0/15:0
CL (63:0)	1337.9466	1337.9488	-1.6114	15:0/15:0/16:0/17:0
CL (64:0)	1351.9622	1351.9644	-1.6317	17:0/17:0/17:0/17:0
Cardiolipins $[M - 2H]^{2-}$				
CL (30:0)	647. 4475			15:0/15:0; 14:0/16
CL (32:0)	661.4632			15:0/15:0; 15:0/17:0
CL (33:0)	667.9647			15:0/15:0; 16:0/17:0
CL (34:0)	675.4785			17:0/17:0; 15:0/19:0; 16:0/18:0
Phosphatidylglycerols $[M + NH_4]^+$				
PG (30:0)	712.5103	712.5123	-2,8070	15:0/15:0
PG (31:0)	726.5256	726.5285	-4,0081	15:0/16:0
PG (32:0)	740.5412	740.5436	-3.2409	15:0/17:0
Phosphatidylethanolamines $[M + H]^+$				
PE (28:0)	636.4575	636.4604	-4.6240	15:0/13:0; 14:0/14:0
PE (29:0)	650.4742	650.4761	-2.8933	15:0/14:0
PE (30:1)	662.4766	662.4761	0.7819	15:1/15:0; 14:0/16:1; 14:1/16:0
PE (30:0)	664.4901	664.4917	-2.4560	15:0/15:0; 14:0/16:0
PE (31:1)	676.4917	676.4917	-0.0473	15:0/16:1
PE (31:0)	678.5055	678.5074	-2.7737	15:0/16:0; 14:0/17:0
PE (32:1)	690.5074	690.5074	0.0261	15:0/17:1; 16:1/16:0
PE (32:0)	692.5208	692.5230	-3.2230	15:0/17:0; 16:0/16:0
PE (33:2)	702.5063	702.5074	-1.5402	15:0/18:2
PE (33:1)	704.5225	704.5230	-0.7551	15:0/18:1; 16:0/17:1;17:0/16:1
PE (33:0)	706.5362	706.5387	-3.5129	15:0/18:0; 17:0/16:0
PE (34:1)	718.5384	718.5387	-0.3925	18:1/16:0; 16:1/18:0
PE (34:0)	720.5520	720.5543	-3.2350	17:0/17:0; 15:0/19:0; 16:0/18:0

651

652 The iso and anteiso C15 and C17 are the most abundant FAs of *B. licheniformis* I89.

653 It is not possible to distinguish the linear C15 and C17 from their branched isomers by

654 LC-MS and MS/MS analysis.

655

656

ACCEPTED MANUSCRIPT

Table 2. Molecular species of glycolipids from *B. licheniformis* I89 identified by LC-MS in positive and negative ion modes

Mass spectrometry data				
Lipid Group	Observed *m/z* value	Calculated *m/z* value	Mass deviation [ppm]	Fatty acid chain
Diglycosyldiacylglycerols $[M + NH_4]^+$				
DGDG (29:0)	868.5975	868.5997	-2.5892	14:0/15:0
DGDG (30:0)	882.6130	882.6154	-2.7181	15:0/15:0;14:0/16:0
DGDG (31:1)	894.6130	894.6154	-2.6816	15:0/16:1
DGDG (31:0)	896.6283	896.6310	-3.0659	15:0/16:0;17:0/14:0
DGDG (32:1)	908.6270	908.6310	-4.4562	15:0/17:1
DGDG (32:0)	910.6430	910.6467	-4.0619	15:0/17:0
DGDG (33:0)	924.6590	924.6623	-3.6219	15:0/18:0;17:0/16:0;19:0/14:0
DGDG (34:0)	938.6750	938.6780	-3.1949	17:0/17:0;19:0/15:0
Diglycosyldiacylglycerols $[M + CH_3COO]^-$				
DGDG (29:0)	909.5792	909.5787	0.5717	14:0/15:0
DGDG (30:0)	923.5946	923.5943	0.2923	15:0/15:0;14:0/16:0
DGDG (31:0)	937.6101	937.6100	0.1280	15:0/16:0,14:0/17:0
DGDG (32:0)	951.6251	951.6256	-0.5569	15:0/17:0
DGDG (33:0)	965.6408	965.6413	-0.4971	16:0/17:0
Monoglycosyldiacylglycerols $[M + NH_4]^+$				
MGDG (29:0)	706.5442	706.5469	-3.8554	14:0/15:0
MGDG (30:0)	720.5600	720.5620	-2.7756	15:0/15:0
MGDG (31:0)	734.5754	734.5777	-3.1311	15:0/16:0
MGDG (32:0)	748.5917	748.5933	-2.1373	15:0/17:0
MGDG (33:0)	762.6069	762.6095	-3.4408	16:0/17:0
MGDG (34:0)	776.6214	776.6252	-4.8595	17:0/17:0
Monoglycosyldiacylglycerols $[M + CH_3COO]^-$				
MGDG (29:0)	747.5257	747.5259	-0.2074	14:0/15:0
MGDG (30:0)	761.5408	761.5415	-0.9258	15:0/15:0
MGDG (31:0)	775.5568	775.5572	-0.4577	15:0/16:0
MGDG (32:0)	789.5723	789.5728	-0.6396	15:0/17:0
MGDG (33:0)	803.5880	803.5885	-0.5662	16:0/17:0

The iso and anteiso C15 and C17 are the most abundant fatty acids of *B. licheniformis* I89. It is not possible to distinguish the linear C15 and C17 from their branched isomers by LC-MS and MS/MS analysis.

663 Table 3. Molecular species of phosphoglyceroglycolipids from *B. licheniformis* I89
664 identified by LC-MS in negative ion modes.

	Mass spectrometry data			
Lipid Group	Observed *m/z* value	Calculated *m/z* value	Mass deviation [ppm]	Fatty acid chain
Diglycosyldiacylglycerols - Phospho- Glycerol $[M - H]^-$				
LTAP (29:0)	1003.5607	1003.5607	0.0369	14:0/15:0
LTAP (30:0)	1017.5760	1017.5763	-0.3076	15:0/15:0
LTAP (31:0)	1031.5915	1031.5920	-0.4488	15:0/16:0
LTAP (32:0)	1045.6083	1045.6076	0.6570	15:0/17:0
Diglycosyldiacylglycerols - Phospho- Glycerol - Alanyl $[M - H]^-$				
LTAP-Ala (30:0)	1088.6089	1088.6134	-4.1585	15:0/15:0
LTAP-Ala (31:0)	1102.6263	1102.6291	-2.5185	15:0/16:0
LTAP-Ala (32:0)	1116.6445	1116.6447	-0,2033	15:0/17:0

665

666 The iso and anteiso C15 and C17 are the most abundant fatty acids of *B. licheniformis*
667 I89. It is not possible to distinguish the linear C15 and C17 from their branched
668 isomers by LC-MS and MS/MS analysis.

ACCEPTED MANUSCRIPT

669

ACCEPTED MANUSCRIPT

Figure captions

Fig. 1. HILIC-ESI-MS chromatograms of total lipid extracts of *B. licheniformis* I89 in (a) negative ion mode and (b) positive ion mode and the retention time (RT) of each polar lipid class. PG: Phosphatidylglycerol, RT 2.3 min; CL: Cardiolipin, RT 2.3 min; LTAP: Lipoteichoic acid primer, RT 2.5 min; DGDG: Diglycosyldiacylglycerol, RT 3.0 min; MGDG: Monoglycosyldiacylglycerol, RT 3.0 min; LTAP-Ala: Mono-alanylated lipoteichoic acid primer, RT 4.0 min; PE: Phosphatidylethanolamine, RT 5.1 min; lys-PG: lysyl-phosphatidylglycerol, RT 15.7 min.

Fig. 2. Chemical structures of the polar lipids identified in *B. licheniformis* I89.

Fig. 3. LC-MS spectra of the phospholipid classes identified in *B. licheniformis* I89 lipidome in the negative ion mode: PG (a), lys-PG (c), CL (e) and in positive ion mode for PE (g). LC-MS/MS spectra and fragmentation pattern of one of the possible isomers of the $[M - H]^-$ ions of PG (17:0/15:0) at *m/z* 721.5 (b), lys-PG (17:0/15:0) at *m/z* 849.6 (d), CL (15:0/15:0/15:0/17:0) at *m/z* 1323.9 (f) and of the $[M + H]^+$ ion of PE (17:0/15:0) at *m/z* 692.3 (h).

Fig. 4. LC-MS spectra of glycolipids identified in *B. licheniformis* I89 lipidome: MGDG (a) and DGDG (c). LC-MS/MS spectra acquired in positive ion mode and fragmentation pattern of one of the possible isomers of MGDG (17:0/15:0) at *m/z* 748.6 (b) and DGDG (17:0/15:0) at *m/z* 910.6 (d).

693 Fig. 5. LC-MS spectra of phosphoglyceroglycolipids identified in *B. licheniformis*
694 I89: LTAP (a) and LTAP-Ala (c). LC-MS/MS spectra acquired in negative ion mode
695 and fragmentation pattern of one of the possible isomers of the $[M - H]^-$ ions LTAP
696 (15:0/15:0) at *m/z* 1017.6 (b) and LTAP-Ala (17:0/15:0) at *m/z* 1116.6 (d).

697

698 Fig. 6. Comparison of the polar lipid species of *B. licheniformis* I89 between the lag,
699 exponential (Exp) and stationary (Sta) growth phases at 37 °C: (a) PG, (b) lys-PG, (c)
700 CL (d) PE, (e) DGDG, (f) MGDGD, (g) LTAP and (h) LTAP-Ala. Values are means
701 ± standard deviation, * $p < 0.05$, *** $p < 0.01$ and *** $p < 0.001$.

ACCEPTED MANUSCRIPT

a) HILIC-ESI-MS – Negative ion mode

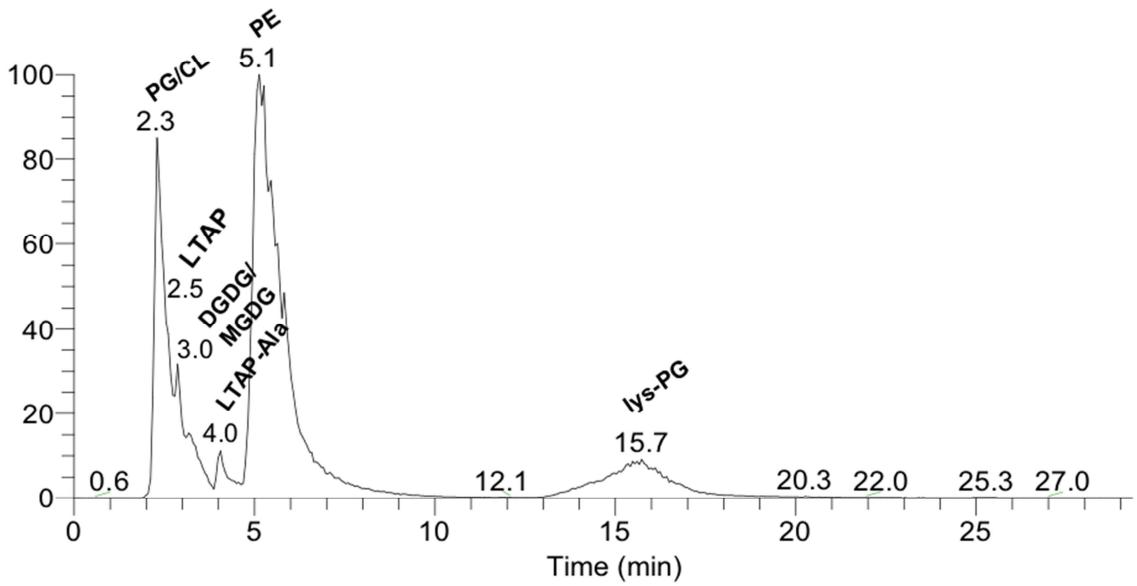

b) HILIC-ESI-MS – Positive ion mode

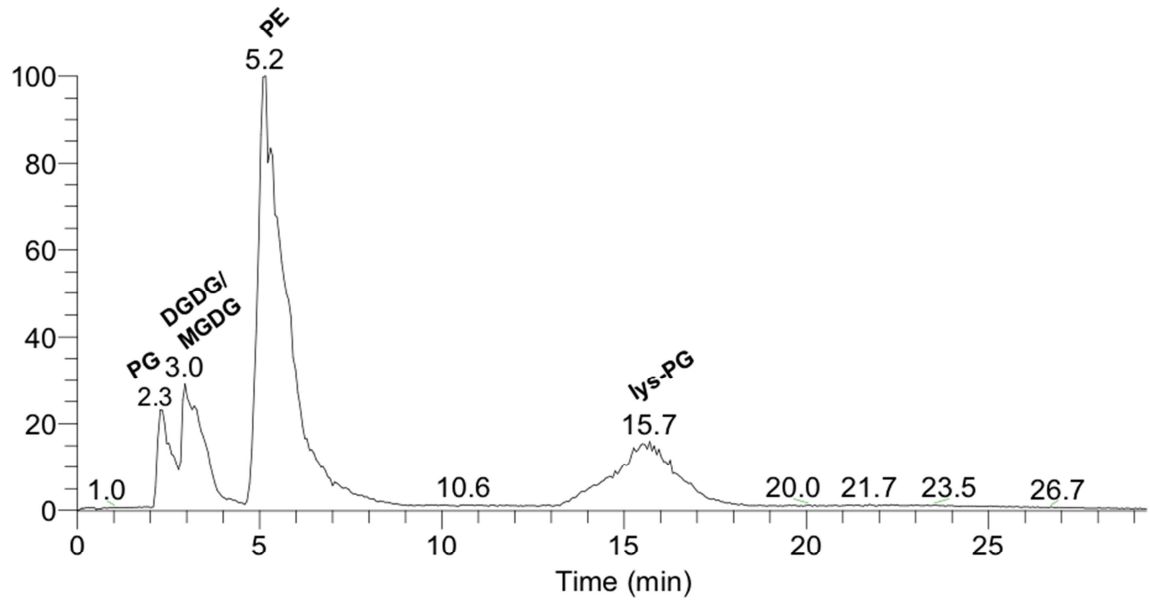

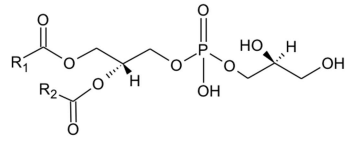

PG- phosphatidylglycerol

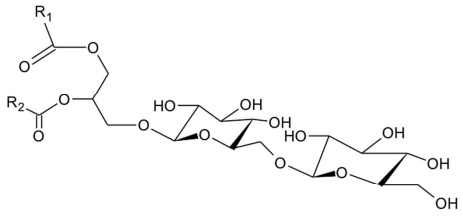

DGDG- diglycosyldiacylglycerol

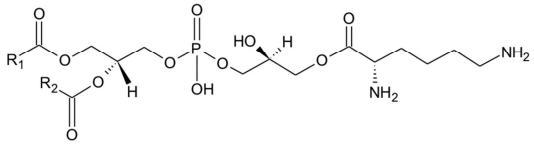

Lysyl-PG - phosphatidylglycerol

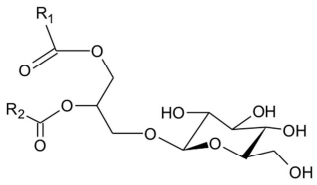

MGDG- monoglycosyldiacylglycerol

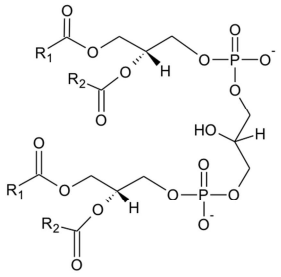

CL- cardiolipin

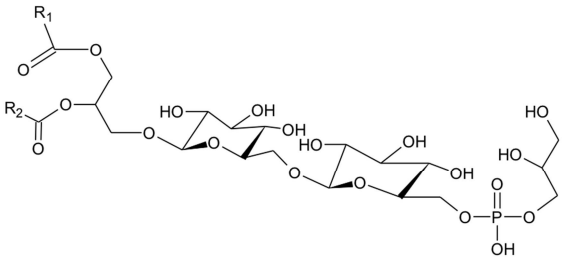

LTAP- lipoteichoic acid primer

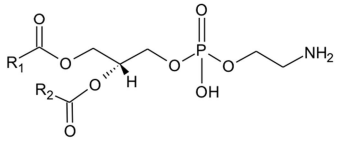

PE- posphatidylethanolamine

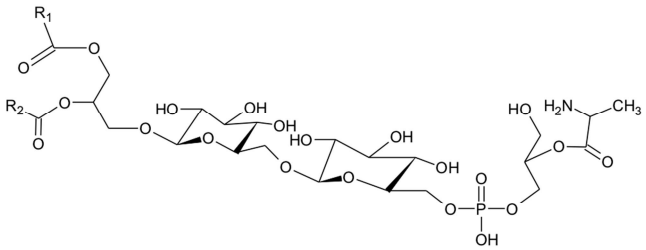

LTAP-Ala- alanyl-lipoteichoic acid primer

ACCEP

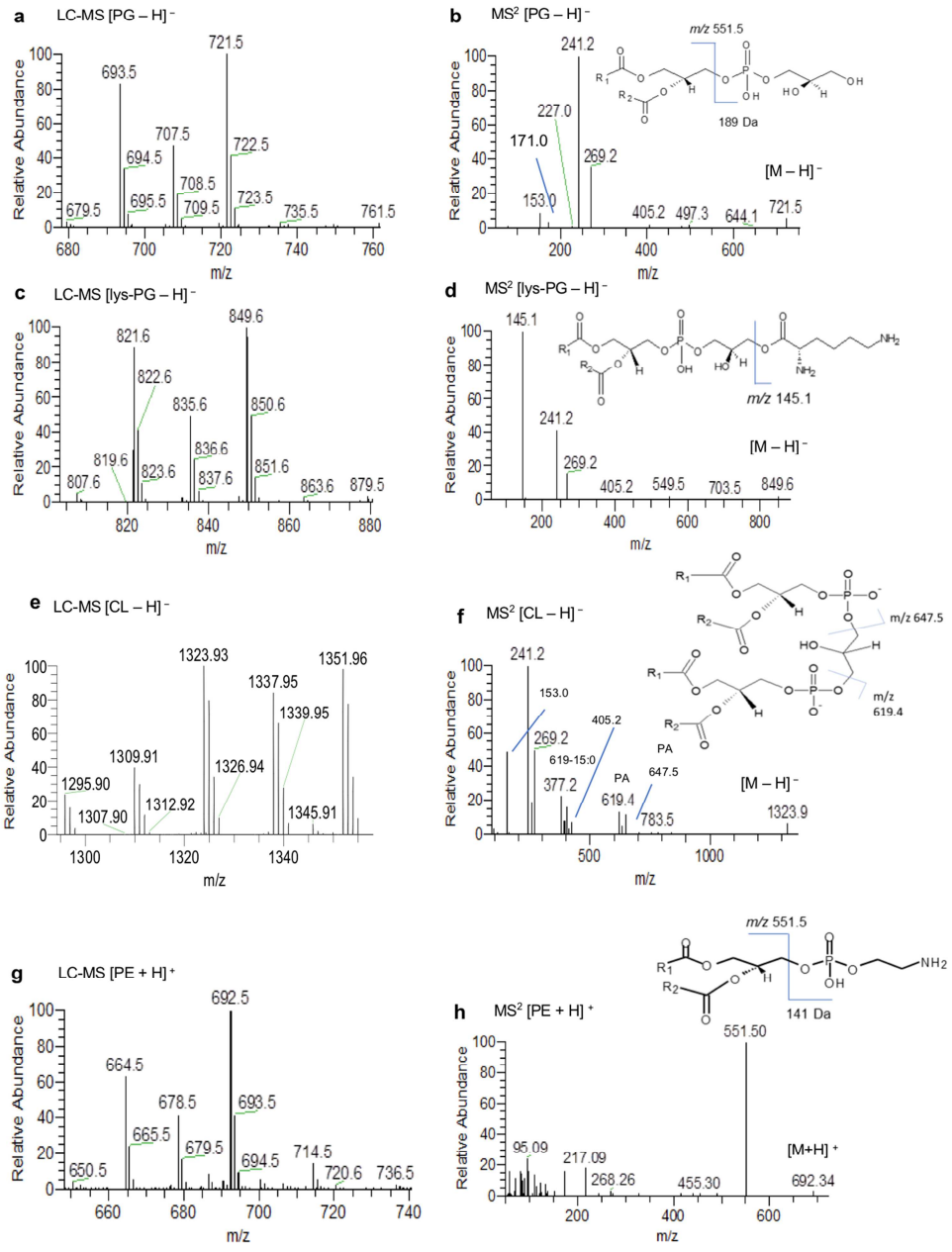
a
LC-MS [PG – H] -
Relative Abundance
m/z
b
MS² [PG – H] -
m/z 551.5
189 Da
[M – H] -
c
LC-MS [lys-PG – H] -
d
MS² [lys-PG – H] -
m/z 145.1
e
LC-MS [CL – H] -
f
MS² [CL – H] -
m/z 647.5
m/z 619.4
PA
619-15:0
[M – H] -
g
LC-MS [PE + H] +
h
MS² [PE + H] +
m/z 551.5
141 Da
[M+H] +

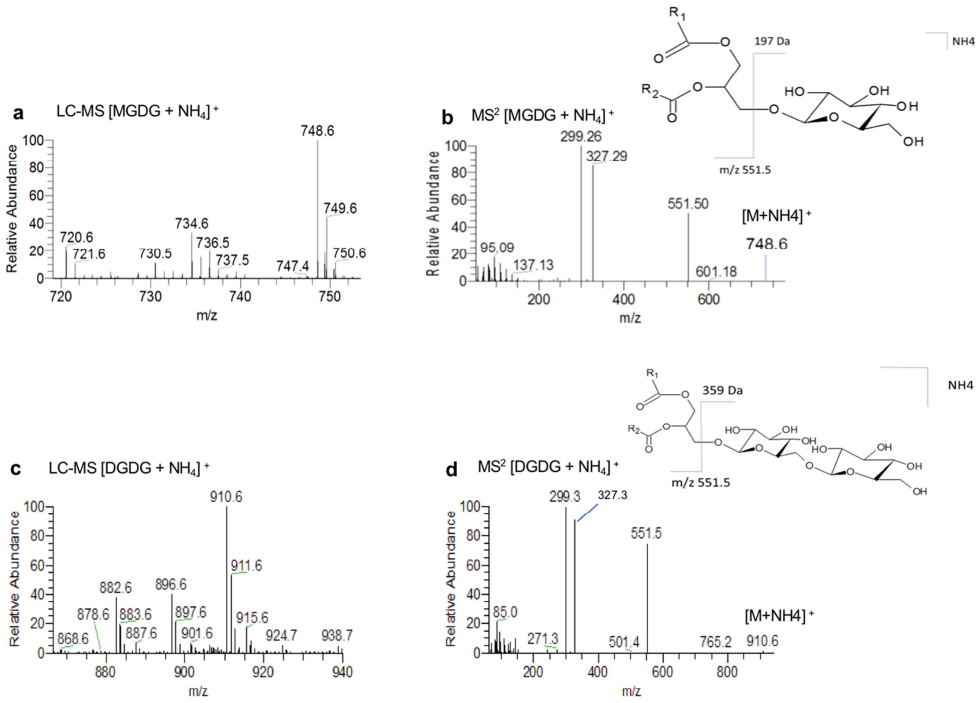
a
LC-MS [MGDG + NH4]+
Relative Abundance
m/z
748.6
749.6
720.6
721.6
730.5
734.6
736.5
737.5
747.4
750.6
b
MS2 [MGDG + NH4]+
299.26
327.29
551.50
[M+NH4]+
748.6
95.09
137.13
601.18
197 Da
NH4
m/z 551.5
c
LC-MS [DGDG + NH4]+
910.6
911.6
882.6
896.6
878.6
883.6
897.6
887.6
901.6
915.6
924.7
938.7
868.6
d
MS2 [DGDG + NH4]+
299.3
327.3
551.5
[M+NH4]+
85.0
271.3
501.4
765.2
910.6
359 Da
NH4
m/z 551.5

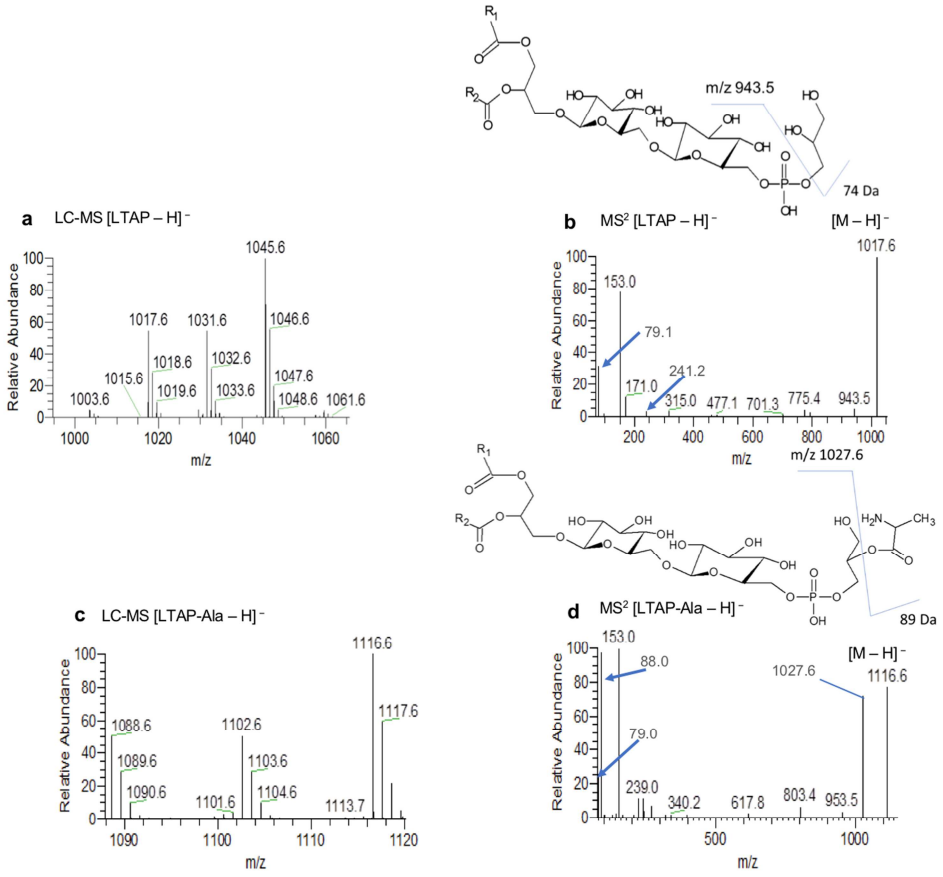
a LC-MS [LTAP – H]⁻
Relative Abundance
m/z
1045.6
1017.6
1031.6
1046.6
1018.6
1032.6
1015.6
1047.6
1019.6
1033.6
1003.6
1048.6
1061.6
b MS² [LTAP – H]⁻
[M – H]⁻
1017.6
153.0
79.1
241.2
171.0
315.0
477.1
701.3
775.4
943.5
m/z 943.5
74 Da
m/z 1027.6
c LC-MS [LTAP-Ala – H]⁻
1116.6
1117.6
1088.6
1102.6
1089.6
1103.6
1090.6
1104.6
1101.6
1113.7
d MS² [LTAP-Ala – H]⁻
153.0
88.0
[M – H]⁻
1027.6
1116.6
79.0
239.0
340.2
617.8
803.4
953.5
89 Da

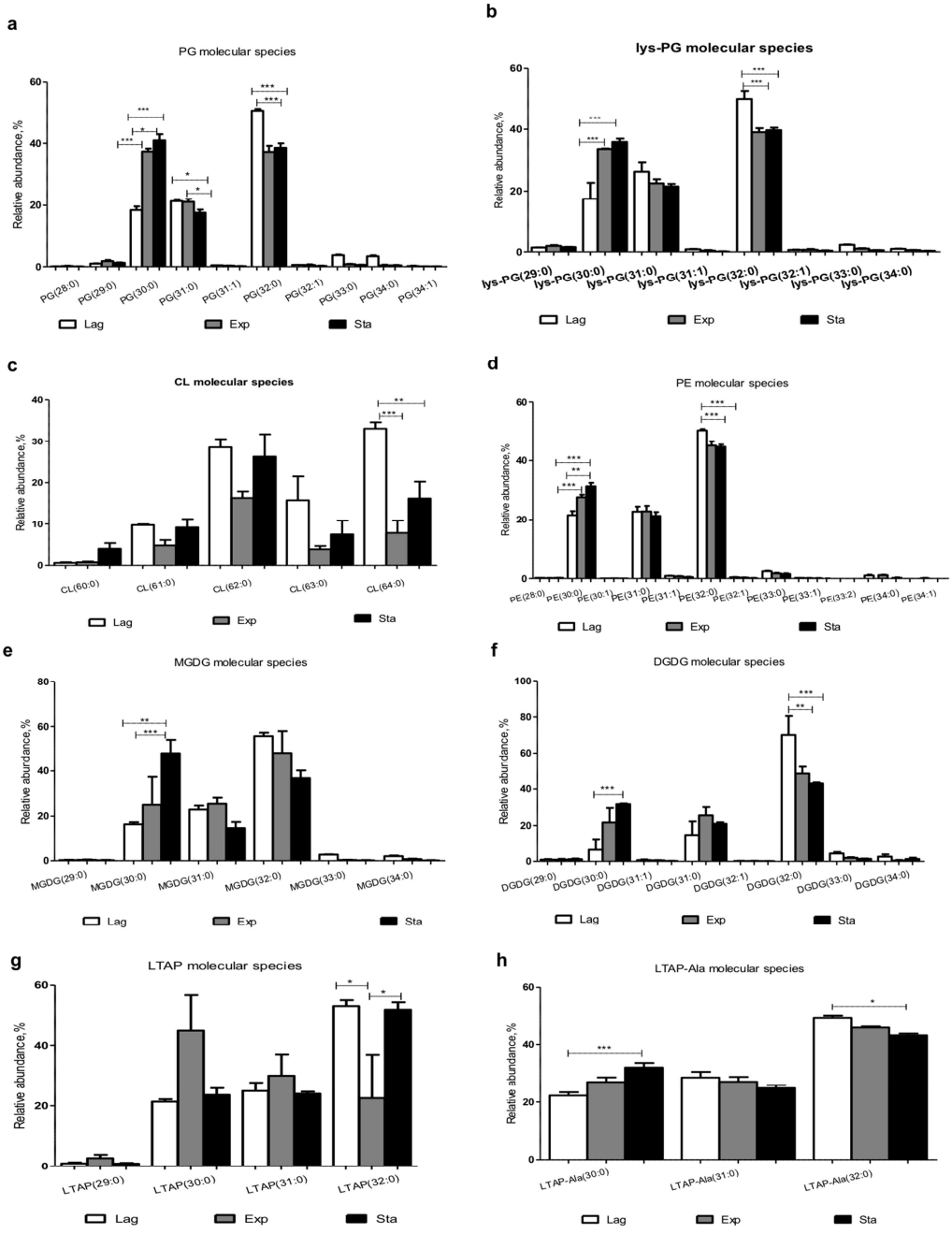
a
PG molecular species
Relative abundance,%
PG(28:0)
PG(29:0)
PG(30:0)
PG(31:0)
PG(31:1)
PG(32:0)
PG(32:1)
PG(33:0)
PG(34:0)
PG(34:1)
Lag
Exp
Sta
b
lys-PG molecular species
Relative abundance,%
lys-PG(29:0)
lys-PG(30:0)
lys-PG(31:0)
lys-PG(31:1)
lys-PG(32:0)
lys-PG(32:1)
lys-PG(33:0)
lys-PG(34:0)
Lag
Exp
Sta
c
CL molecular species
Relative abundance,%
CL(60:0)
CL(61:0)
CL(62:0)
CL(63:0)
CL(64:0)
Lag
Exp
Sta
d
PE molecular species
Relative abundance,%
PE(28:0)
PE(30:0)
PE(30:1)
PE(31:0)
PE(31:1)
PE(32:0)
PE(32:1)
PE(33:0)
PE(33:1)
PE(33:2)
PE(34:0)
PE(34:1)
Lag
Exp
Sta
e
MGDG molecular species
Relative abundance,%
MGDG(29:0)
MGDG(30:0)
MGDG(31:0)
MGDG(32:0)
MGDG(33:0)
MGDG(34:0)
Lag
Exp
Sta
f
DGDG molecular species
Relative abundance,%
DGDG(29:0)
DGDG(30:0)
DGDG(31:1)
DGDG(31:0)
DGDG(32:1)
DGDG(32:0)
DGDG(33:0)
DGDG(34:0)
Lag
Exp
Sta
g
LTAP molecular species
Relative abundance,%
LTAP(29:0)
LTAP(30:0)
LTAP(31:0)
LTAP(32:0)
Lag
Exp
Sta
h
LTAP-Ala molecular species
Relative abundance,%
LTAP-Ala(30:0)
LTAP-Ala(31:0)
LTAP-Ala(32:0)
Lag
Exp
Sta

ACCEPTED MANUSCRIPT

Highlights

- *B. licheniformis* I89 lipidome was characterized by HILIC–ESI–MS, mass accuracy and MS/MS.
- Phospholipids included phosphatidylethanolamines, phosphatidylglycerols, lysyl-PG and cardiolipins.
- Glycolipids included monoglycosyldiacylglycerols and diglycosyldiacylglycerols.
- Phosphoglyceroglycolipids comprised lipoteichoic acid primer (LTAP) and mono-alanylated LTAP.
- The polar lipidome changed significantly among the growth phases at 37 °C.

ACCEPTED MANUSCRIPT